

Coupled Effects of Porous Medium Layer and Micro-Polar Lubricants on Transient Squeeze Elastohydrodynamic Lubrication

Li-Ming Chu*, Chang-Jian, Cai-Wan** and Yuh-Ping Chang***

Keywords : Porous medium layer, micro-polar lubricants, EHL, transient Squeeze

ABSTRACT

A numerical manner is expanded to calculate transient film thicknesses, pressures, and normal squeeze velocities during transient squeeze process in an isothermal elastohydrodynamic lubrication (EHL) spherical conjunction using micro-polar (MP) lubricants with porous medium layer (PML) for fixed loading. The transient modified Reynolds equation is obtained using Darcy's law and Eringen's micro-polar rheology according to cylinder coordinates. The coupled transient modified Reynolds, lubricant rheology, load balance, and elasticity deformation equations are solved simultaneously by means of finite difference method (FDM), successive over-relaxation method (SORM) and Gauss-Seidel iteration method (GSIM). The simulation results revealed that the influence of PML is equal to absorb lubricant, so film thickness is reduced. The influence of MP lubricant is equal to enhance lubricant viscosity, so film thickness is enlarged during transient pure squeeze process. Due to variation of film thicknesses, the pressure distributions change in different zones for fixed loading. The influences of thickness and permeability of PML as well as characteristic length and coupling parameter of MP lubricant are discussed.

INTRODUCTION

The different types of lubricant additives are entered into base lubricant to improve durability of friction parts and reduce friction between contact

Paper Received November, 2023. Revised January, 2024. Accepted April, 2024. Author for Correspondence: Yuh-Ping Chang.

* *Professor, Department of Green Energy and Information Technology, National Taitung University, Taitung City 950309, Taiwan, ROC*

** *Department of Mechanical Engineering, National Chin-Yi University of technology, Taichung City 411030, Taiwan, R.O.C.*

*** *Department of Mechanical Engineering, Kun Shan University, Tainan City 710303, Taiwan, R.O.C.*

surfaces. Due to self-included oil storage and low friction characteristics, porous bearings have been widely used in industry. During squeeze process, high pressure results in elastic deformation between contact zones. Therefore, the influences of PML and MP lubricants on squeeze EHL motion are worth discussing.

In recent years, Sakim et al. (2018) studied numerically finite porous elastic journal bearings (JB) performance using couple stresses fluid and Darcy's law, but they considered bearing elastic deformation using Winkler model (1867). Shah and Kataria (2016) derived transient modified Reynolds equation in polar coordinates by means of ferrohydrodynamics theory and Darcy's law theory to study a rigid sphere squeezing a rigid flat plate with porous layer. The squeeze film and pressure were calculated numerically for different parameter. The results showed that the system performs better when ferrofluid was used as lubricant. Rahul and Rao (2021) studied the influences of PML and Rabinowitsch lubricants on an isothermal hydrodynamic lubrication (HL) of circular stepped plates with surface roughness (SRN) under pure extrusion motion. They compared transient characteristic of circular stepped with and without surface roughness, porous medium layer, viscosity, and roughness pattern. Many studies (Kalavathi et al., 2016, Boubendir et al., 2019) researched the lubrication performances of porous JB using different lubricants and SRN patterns, but elastic deformation phenomenon did not be considered. They thought that permeability of PML has important influences on porous bearings.

When contact pairs generate high pressure in contact zone due to squeeze motion, the elastic concave occurs in many lubricated mechanical elements. Squeeze phenomenon are observed in many areas of real life. Many researchers (Chu et al., 2020, Yang and Wen, 1991, Venner et al., 2016) investigated EHL Spherical Conjunctions for fixed loading at squeeze action. The oil pocket was formed due to high pressures cause elastic deformation during squeeze process. Many researchers

(Dowson and Wang, 1994, Larsson and Höglund, 1995) analyzed transient pressure distribution and film thickness shape of an elastic sphere crashing and rebounding on an oily plate. Most related studies (Yang and Wen, 1991, Venner et al., 2016, Dowson and Wang, 1994, Larsson and Höglund, 1995) used Newtonian fluid to analyze squeeze characteristics of EHL.

In order to improve lubrication performance, lubricating additives have been widely used in industries. Many micro-continuum theorems have been presented to analyze additives efficiencies. Chetti (2014) used Eringen's (1966) MP fluid theory to investigate static characteristics for deformable shell and rigid shaft of JB lubricated using Newtonian and MP fluids. Das and Guha (2016) explored numerically HD characteristics of finite JB using MP lubrication in turbulent reign. They found that the disorder of MP lubrication has a detrimental influence for whirl ratio and stability. Halambi and Hanumagowda (2018) analyzed theoretically lubrication performances of MP fluid between two elliptic plates with a magnetic field. They thought that conducting MP fluid increases load capacity and extrusion time. However, the study of MP lubricant with PML on EHL point conjunction for squeeze action is inadequate. So this issue is necessary for further exploration.

This paper investigates the MP lubricant between elastic sphere and PML on squeeze EHL action for fixed loading. The FDM, SORM, and GSIM are used to analyze squeeze EHL characteristics of PML and MP lubricants with time.

THEORETICAL ANALYSIS

The elastic ball is squeezing an infinite rigid flat with PML for fixed loading, as shown in Fig. 1. The compressible MP lubricant is filled between elastic ball and PML. The reduced momentum equations and continuity equation governing motion of lubricant given in polar coordinates using Eringen's [13] MP fluid theory for usual assumption of EHL applicable to a thin film can be obtained as:

$$\frac{\partial p}{\partial r} = \frac{1}{2}(2\mu + \chi) \frac{\partial^2 u}{\partial z^2} + \chi \frac{\partial v_y}{\partial z} \quad (1)$$

$$\gamma \frac{\partial^2 v_y}{\partial z^2} - \chi \frac{\partial u}{\partial z} - 2\chi v_y = 0 \quad (2)$$

$$\frac{\partial p}{\partial z} = 0 \quad (3)$$

$$\frac{1}{r} \frac{\partial(\rho r u)}{\partial r} + \frac{\partial \rho w}{\partial z} = 0 \quad (4)$$

Where v_y is micro rotational velocity, χ and γ are additional viscosity coefficients for MP fluids.

The velocity boundary conditions (B.C.) at surfaces of elastic ball and PML are:

$$u(r,0) = 0, \quad v_y(r,0) = 0, \quad w(r,0) = w^* \quad (5)$$

$$u(r,h) = 0, \quad v_y(r,h) = 0, \quad w(r,h) = \frac{\partial h}{\partial t} \quad (6)$$

Where w^* is modified Darcy velocity in PML. The MP lubricant is determined by Darcy's law in PML given by

$$w^* = \frac{-k}{(\mu + \chi)} \frac{\partial p^*}{\partial z} \quad (7)$$

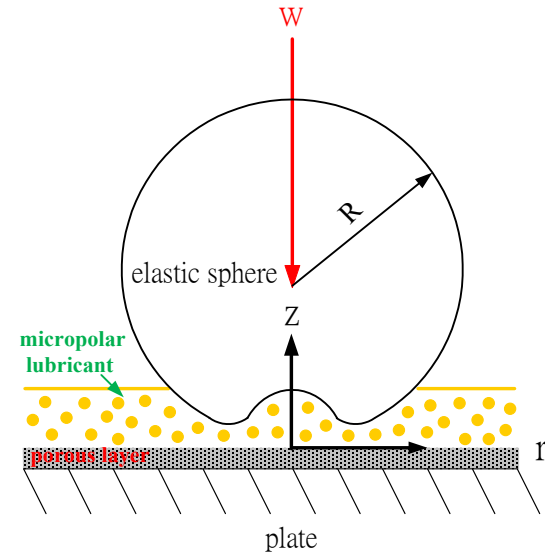


Fig. 1 Geometry of EHL under pure squeeze motion with MP lubricant and PML

Due to fluid motion continuity in PML, the p^* (pressure) satisfies the Laplace equation.

$$\frac{1}{r} \frac{\partial}{\partial r} \left(r \frac{\partial p^*}{\partial r} \right) + \frac{\partial^2 p^*}{\partial z^2} = 0 \quad (8)$$

The B.C. are:

$$z = -\delta, \quad \frac{\partial p^*}{\partial z} = 0 \quad (9)$$

$$z = 0, \quad p = p^* \quad (10)$$

Integrating Eq. (8) across thickness of PML using boundary conditions, pressure gradient at $z=0$ can be obtained. Substituting it into Eq. (7), w^* can be obtained as:

$$w^*(z=0) = \frac{k\delta}{r(\mu + \chi)} \frac{\partial}{\partial r} \left(r \frac{\partial p}{\partial r} \right) \quad (11)$$

The velocities at surface of PML and sphere are zero. Integrate equations (1)-(3) using B.C., u can be obtained as:

$$u(r,z) = \frac{z^2}{2\mu} \frac{dp}{dr} + Nl \frac{h}{2\mu} \frac{dp}{dr} \left[\sinh\left(\frac{Nz}{l} - \frac{z}{lN}\right) - \coth\left(\frac{Nh}{2l}\right) \cosh\left(\frac{Nz}{l} - 1\right) \right] \quad (12)$$

Where

$$l = \left(\frac{\gamma}{4\mu}\right)^{1/2}, \quad N = \left(\frac{\chi}{2\mu + \chi}\right)^{1/2}$$

Substituting w^* and u into continuity equation and integrating z from 0 to h with w^* and $w(r, h) = \partial h / \partial t$, transient modified Reynolds equation in polar coordinates can be derived as:

$$\frac{\partial}{\partial r} \left\{ \frac{\rho r}{\mu} [(h^3 + 12hl^2 - 6Nlh^2) \coth(\frac{Nh}{2l}) + \frac{12 \mu \kappa \delta}{(\mu + \chi)}] \frac{\partial p}{\partial r} \right\} = 12 r \frac{\partial \rho h}{\partial t} \quad (13)$$

The equation (13) can be obtained in dimensionless form:

$$\frac{\partial}{\partial X} \left(\frac{\bar{\rho} H^3 X}{\bar{\mu}} [1 + 12(\frac{L}{H})^2 - 6N(\frac{L}{H})] \coth(\frac{NH}{2L}) + \frac{12 \bar{\mu} K \bar{\delta}}{(\bar{\mu} + \bar{\chi}) H^3} \right) \frac{\partial P}{\partial X} = KX \frac{\partial(\bar{\rho} H)}{\partial T} \quad (14)$$

The B.C. for equation (14) are:

$$P(X \rightarrow \infty, T) = 0 \quad (15a)$$

$$\frac{\partial}{\partial X} P(0, T) = 0 \quad (15b)$$

$$P(R, T) \geq 0 \quad (15c)$$

In high pressure area, the relationship between density and pressure (1966) is expressed as:

$$\bar{\rho} = \frac{\rho}{\rho_0} = 1 + \frac{0.6 \times 10^{-9} p}{1 + 1.7 \times 10^{-9} p} \quad (16)$$

The relationship between viscosity and pressure (1963) is expressed as:

$$\bar{\mu} = \exp\{(9.67 + \ln \mu_0)[-1 + (1 + 5.1 \times 10^{-9} p)^{-1}]\} \quad (17)$$

The film thickness in EHL sphere conjunction can be expressed as:

$$\bar{h}(r, t) = \bar{h}_0(t) + \frac{r^2}{2R} + \Delta(r, t) \quad (18)$$

The dimensionless form of equation (18) can be obtained as:

$$\bar{H}_i = \bar{H}_0 + \frac{X_i^2}{2} + \bar{\Delta}(X, T) \quad (19)$$

According to superposition theorem for elastic systems, the deformation can thus be computed at discrete points i as a sum of deformation contributions from all pressure points j :

$$\bar{\Delta}_i = \sum_{j=1}^n D_{ij} P_j \quad (20)$$

where D_{ij} is influence coefficients.

The load balance equation for fixed loading is

$$\int_0^\infty PX dX = \frac{1}{3} \quad (21)$$

RESULTS AND DISCUSSION

To explore the influences of MP lubricant between elastic sphere and PML for fixed loading during squeeze process. The equation (21) must be included in coupled equations (14), (16), (17), and (19).

These equations are solved simultaneously to obtain nodal pressures (P) and film thicknesses (H) with time using parameters listed in Table 1. The initial falling height of ball is $h_{00} = 20 \mu m$. The computational zone in the beginning is chosen as $X_{max} = 16.0$. The uniform grid is made up of 401 nodes in every calculation domain. The FDM, GSIM, and SORM are employed to calculate H and P at each time step. The typical problem with $\Psi = 1.048 \times 10^{-8}$, $K = 3.1743 \times 10^{-4}$, $\bar{\delta} = 7.9678 \times 10^{-2}$, $G = 3500$, $L = 7.9678 \times 10^{-3}$, and $N = 0.5$ is solved. Figure 2 shows flow chart.

Table 1 Computational data.

Properties of lubricants	
G (Material parameter)	3500
Inlet viscosity of lubricant, Pa-s	0.04
Inlet density of lubricant, kg/m ³	846
Pressure viscosity coefficient, 1/GPa	15.91
Pressure-viscosity index (Roelands)	0.4836
Properties of balls	
Reduced radius, m	0.02
Density of balls, kg/m ³	7850
Elastic modulus of balls, GPa	200
Poisson's ratio of balls	0.3

Figure 3 displays P and H in X-axis calculated using present model and classical EHL model with $\Psi = 1.048 \times 10^{-8}$, $K = 3.1743 \times 10^{-4}$, $G = 3500$, $\bar{\delta} = 7.9678 \times 10^{-2}$, $L = 7.9678 \times 10^{-3}$, and $N = 0.5$. The P is quite flat at relatively large H, but it becomes steeper with decreasing H. As shown, peak pressure always remained in center. The initial changes are more obvious. Subsequent changes are more gradual. The influence of PML is equal to absorb lubricants during squeeze process. Therefore, H is decreased. The influence of MP lubricant is equal to enhance lubricant viscosity, so H is enlarged. The influence of PML is more obvious in this case. Thus, H is reduced. The P of MP lubricant with PML is larger than those of Newtonian (NW) lubricants under same load and time in central zone. However, the P of present model is smaller than that of NT lubricant in middle zone, the P of present model is larger than that of NW lubricant near exit zone due to fixed loading.

Figure 4 displays P and H in X-axis calculated using present model and classical EHL model with $\Psi = 1.048 \times 10^{-8}$, $K = 3.1743 \times 10^{-4}$, $G = 3500$, $\bar{\delta} = 7.9678 \times 10^{-2}$, $L = 39.839 \times 10^{-3}$, and $N = 0.9$. The trends of P and H with time are similar to those shown in Figure 3. The influence of MP lubricant is more obvious. Thus, H is enlarged. The P of MP lubricant with PML is greater than those of NW lubricants for fixed loading and time in central zone. However, the P of present model is smaller than that

of NW lubricant in middle zone, the P of present model is larger than that of NW lubricant near exit zone due to fixed loading.

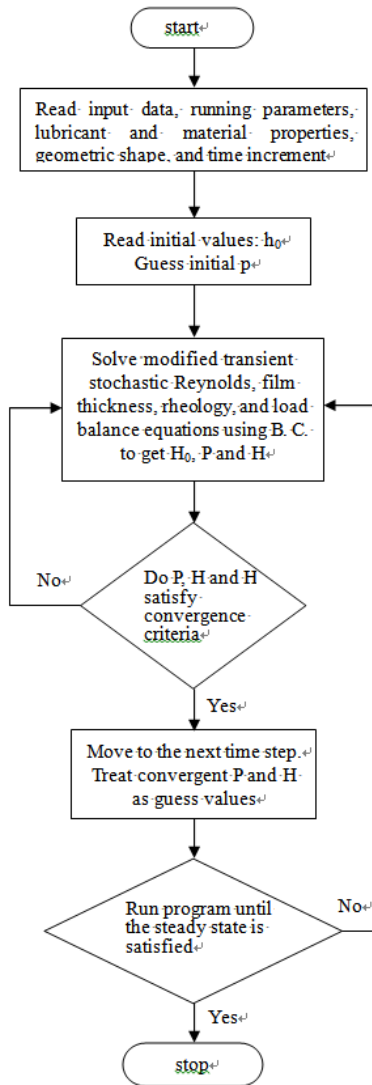


Fig. 2 Flow diagram of computational procedure

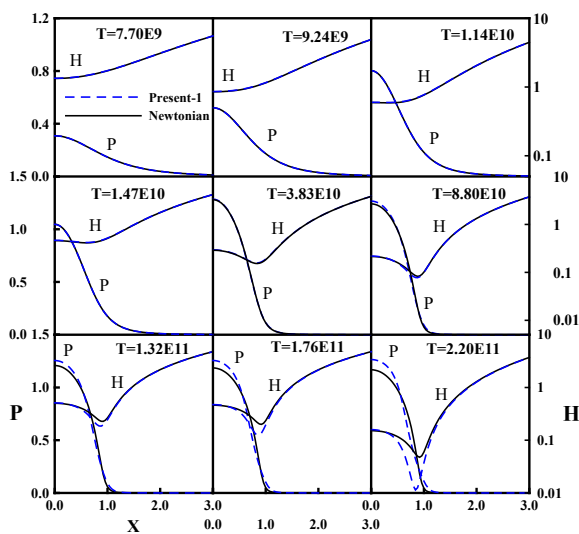


Fig. 3 P and H versus time for $K = 6.3486 \times 10^{-4}$,

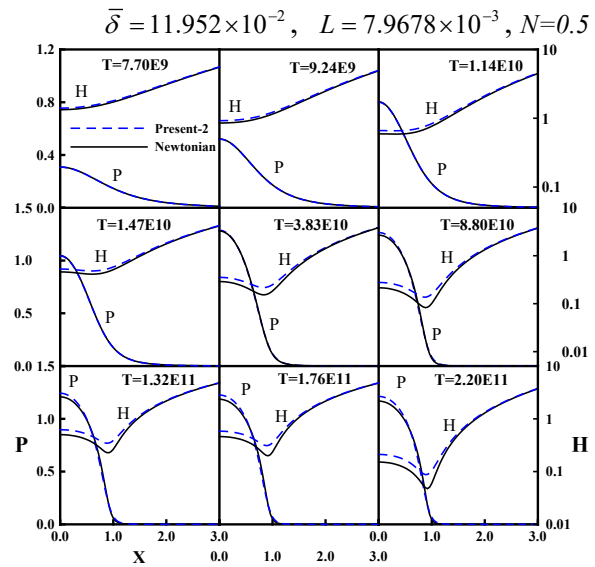


Fig. 4 P and H versus time for $K = 6.3486 \times 10^{-4}$, $\bar{\delta} = 11.952 \times 10^{-2}$, $L = 7.9678 \times 10^{-3}$, $N=0.5$

Figure 5 displays P and H in X-axis calculated using present model for different K and $\bar{\delta}$ with $\Psi = 1.048 \times 10^{-8}$, $L = 7.9678 \times 10^{-3}$, $G = 3500$, $T = 2.2022 \times 10^{11}$, and $N=0.5$. As shown in Figure 3, due to squeeze influences, very high pressure is generated in lubricating film. Therefore, an elastic concave occurs at contact zone, increased gradually to a maximum value, and then concave decreased gradually to H_{min} with X-axis. The PML absorbs lubricant due to squeezing effect, so H will decrease, P will increase or decrease in different areas for fixed loading. The greater K and $\bar{\delta}$ of PML, the greater adsorption effect of PML. The H become smaller due to PML absorbed lubricants. The greater the K, the smaller the H, the larger the P in central zone, the smaller the P in middle zone, and the larger the P in exit zone for same PML thickness and MP lubricant.

The larger the $\bar{\delta}$ value, the smaller the H, the larger the P in central zone, the smaller the P in middle zone, and the larger the P in exit zone for same K value and MP lubricant.

Figure 6 shows P_c , H_c , and H_{min} versus time for different K and $\bar{\delta}$ with $\Psi = 1.048 \times 10^{-8}$, $L = 7.9678 \times 10^{-3}$, $N=0.5$, and $G = 3500$. The P_c increase quickly to a maximum and the H decrease quickly with time in primary stage. They decrease gently to approximate Hertzian contact with time at final stage. The larger the K value, the smaller the H, and the larger the P_c . The larger the $\bar{\delta}$ value, the smaller the H, and the larger the P_c . The times required to reach maximum central pressure (P_{cmax}) and Hertzian pressure (P_{hertz}) increase with increasing K and $\bar{\delta}$.

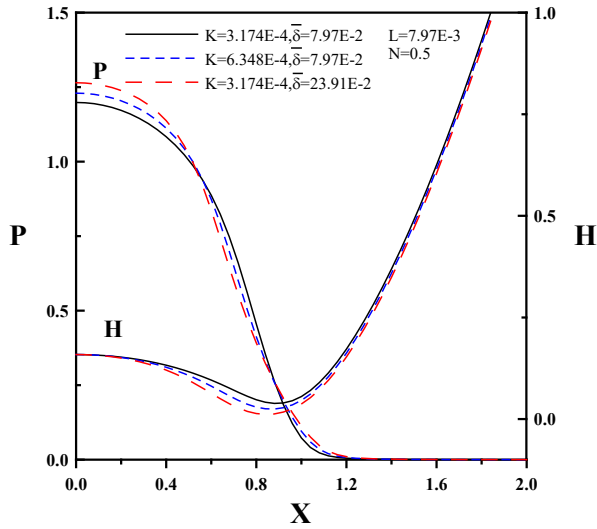


Fig. 5 P and H for different K and $\bar{\delta}$.

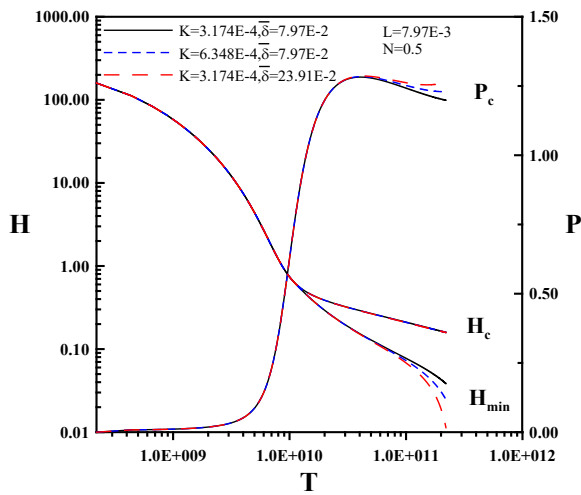


Fig. 6 P_c and H versus time using MP with PML model for different K, $\bar{\delta}$

Figure 7 displays P and H in X-axis calculated using present model for different L and N with $\Psi = 1.048 \times 10^{-8}$, $K = 3.1743 \times 10^{-4}$, $G = 3500$, $\bar{\delta} = 7.9678 \times 10^{-2}$, and $T = 2.2022 \times 10^{11}$. The greater L and N of MP lubricant, the greater the viscosity effect of MP lubricant, so H is enlarged, P will increase or decrease in different areas for fixed loading. The larger the L, the larger the H, the larger the P in central zone, the smaller the P in middle zone, and the larger the P in exit zone for same PML parameters and N. The larger the N, the larger the H, the smaller the P in central zone, the larger the P in middle zone, and the smaller the P in exit zone for same PML parameters and L.

Figure 8 displays P_c , H_c , and H_{min} versus time for different L and N with $\Psi = 1.048 \times 10^{-8}$, $K = 3.1743 \times 10^{-4}$, $\bar{\delta} = 7.9678 \times 10^{-2}$, and $G = 3500$. The changing trends of P and H with time are similar to Figure 6. The larger the L, the larger the H, and the

larger the P_c . The larger the N, the larger the H, and the smaller the P_c . The times required to reach $P_{c_{max}}$ and P_{hertz} increase with increasing L. The times required to reach $P_{c_{max}}$ and P_{hertz} decrease with increasing N.

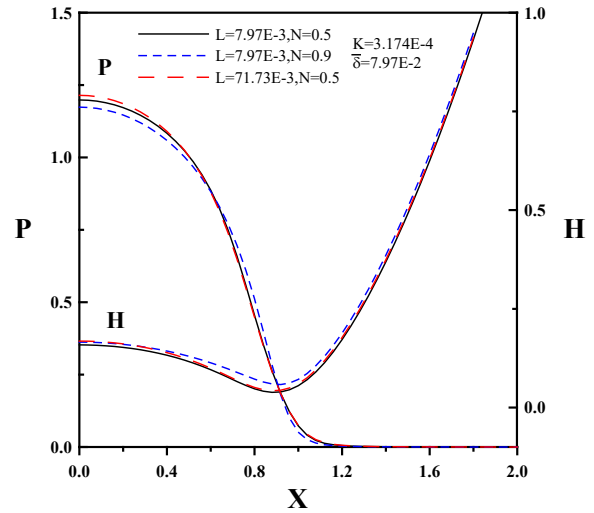


Fig. 7 P and H for different L and N.

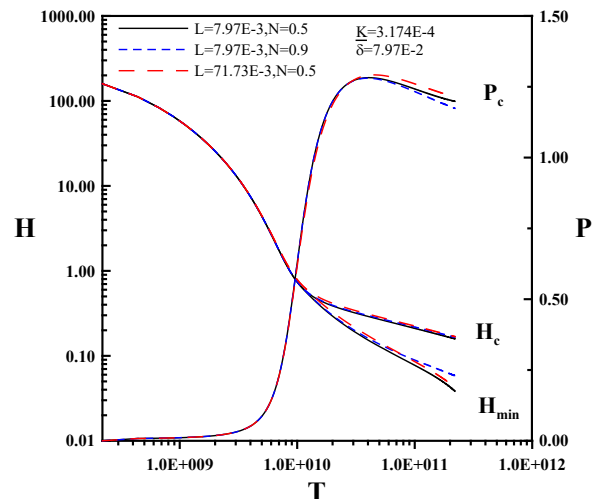


Fig. 8 P_c and H versus time using MP with PML model for different L and N.

Figure 9 displays $P_{c_{max}}$ and least minimum film thickness ($H_{min_{min}}$) during transient pure squeeze process versus K. As mentioned above, the greater K and $\bar{\delta}$ of PML, the greater adsorption effect of PML. Therefore, the larger the K, the smaller the $H_{min_{min}}$, the larger the $P_{c_{max}}$. Figure 10 displays $P_{c_{max}}$ and $H_{min_{min}}$ during transient pure squeeze process versus $\bar{\delta}$. The larger the $\bar{\delta}$, the larger the $P_{c_{max}}$, the smaller the $H_{min_{min}}$.

Figure 11 displays $P_{c_{max}}$ and $H_{min_{min}}$ during transient pure squeeze process versus L. As mentioned above, the greater L and N of MP lubricant, the greater the viscosity effect of MP lubricant. The larger the L, the larger the $P_{c_{max}}$, the larger the $H_{min_{min}}$. Figure 12 displays $P_{c_{max}}$ and $H_{min_{min}}$ during transient pure

squeeze process versus N. The larger the N, the larger the Hmin_{min}. the smaller the Pc_{max}.

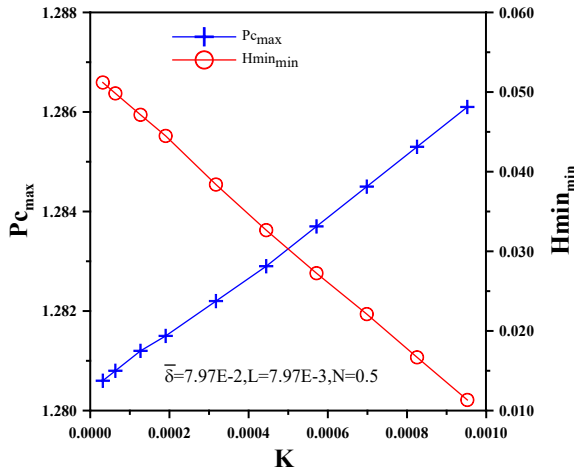


Fig. 9 Pc_{max} and Hmin_{min} versus K.

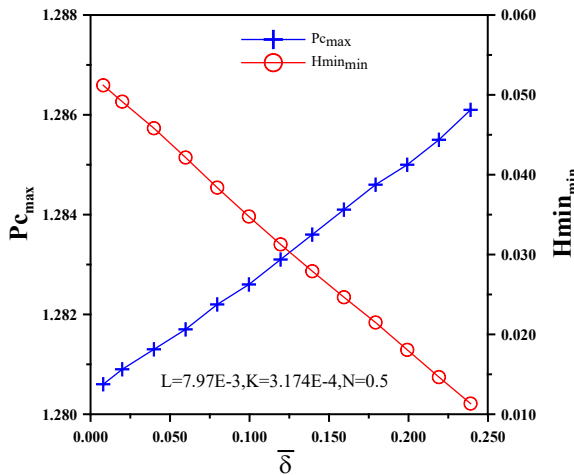


Fig. 10 Pc_{max} and Hmin_{min} versus $\bar{\delta}$.

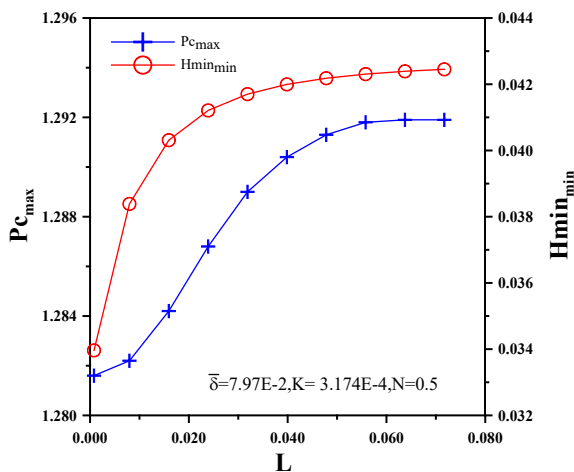


Fig. 11 Pc_{max} and Hmin_{min} versus L.

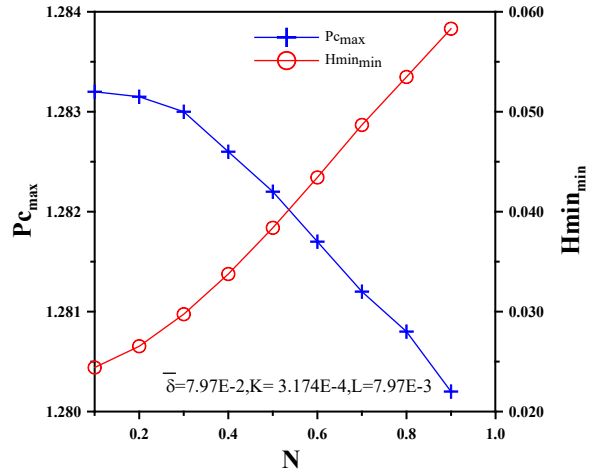


Fig. 12 Pc_{max} and Hmin_{min} versus N.

Figure 13 displays minimum normal squeeze velocity (V_{min}) vs. time for different N, $\bar{\delta}$, L, K. The magnitudes of V_{min} decrease quickly with time at primary period, and magnitudes of V_{min} decrease gently with time at other periods. Due to squeeze, elastic deformation, MP lubricant, and PML influences, the magnitude of V_{min} increases with increasing K, the magnitude of V_{min} increases with increasing $\bar{\delta}$, the magnitude of V_{min} increases with increasing L, the magnitude of V_{min} decreases with increasing N.

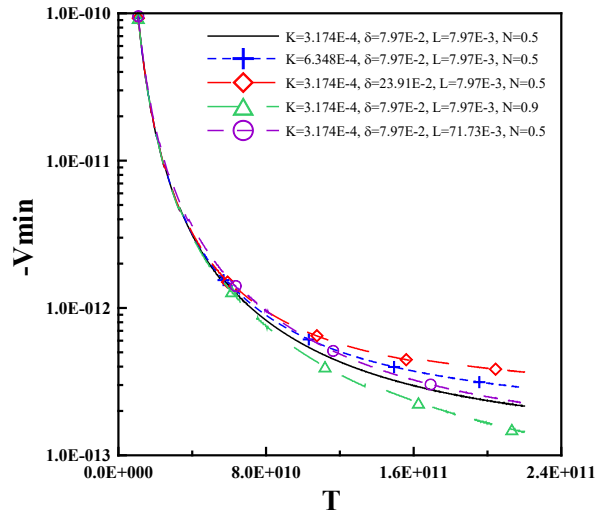


Fig. 13 V_{min} versus T using present model for different K, $\bar{\delta}$, L, N.

CONCLUSIONS

A numerical manner is expanded to investigate the influences of PML and MP lubricants in EHL spherical conjunction for fixed loading under pure squeeze action. During transient pure squeeze process, the influence of PML is equal to absorb lubricants, so film thickness is reduced. The influence of MP

lubricant is equal to enhance lubricant viscosity, so film thickness is increased. Due to variation of film thickness, the pressure distributions change in different zones for fixed loading. The conclusions include:

1. The P_c increase quickly to a maximum and the H decrease quickly with time in primary stage. They decrease gently to approximate Hertzian contact with time at final stage. The peak pressure always remained in center. The elastic concave occurs at central zone.
2. The H of MP lubricant is larger than those of NW lubricant, the H of PML is larger than those of NW lubricant, and the P also change accordingly for fixed loading.
3. The larger the K and $\bar{\delta}$ value, the larger the $P_{C_{max}}$, the smaller the $H_{min_{min}}$. The times required to reach $P_{C_{max}}$ and P_{hertz} increase with increasing K and $\bar{\delta}$.
4. The larger the L value, the larger the $P_{C_{max}}$, the larger the $H_{min_{min}}$. The times need to achieve $P_{C_{max}}$ and P_{hertz} increase with increasing L .
5. The larger the N value, the larger the $H_{min_{min}}$, the smaller the $P_{C_{max}}$. The times need to achieve $P_{C_{max}}$ and P_{hertz} decrease with increasing N .
6. The magnitude of V_{min} increases with increasing K , $\bar{\delta}$, and L . The magnitude of V_{min} decreases with increasing N .

ACKNOWLEDGMENT

The authors express their appreciation to the National Science and Technology Council (NSTC 112-2221-E-143-003) in Taiwan, R.O.C. for financial support. We declare no conflict of interests regarding the publication of this article.

REFERENCES

- Boubendir S, Larbi S, Malki M, Bennacer R. Hydrodynamic self-lubricating journal bearings analysis using Rabinowitsch fluid lubricant, *Tribology International*, 2019; 140:105856.
- Chetti B. Analysis of a circular journal bearing lubricated with micropolar fluids including EHD effects, *Industrial Lubrication and Tribology*, 2014; 66(2):168-173.
- Chu LM, Chang YP, Hsu HC. Effects of surface roughness on transient squeeze EHL motion of circular contacts with micropolar fluids, *Microsystem Technologies*. 2020; 26(9):2903-2911.
- Das S, Guha SK. Turbulent Effect on the Dynamic Response Coefficients of Finite Journal Bearings Lubricated with Micropolar Fluid, *Procedia Technology*, 2016; 23:193-200.
- Dowson D, Higginson GR. *Elastohydrodynamic Lubrication*, Pergamon Press, 1966; 88-92.

- Dowson D, Wang D. An Analysis of the Normal Bouncing of a Solid Elastic Ball on an Oily Plate, *Wear*, 1994; 179:29-37.
- Eringen, AC. Theory of Micropolar Fluids, *Journal of Mathematics and Mechanics*, 1966; 16(1):1-18.
- Halambi B, Hanumagowda BN. effect of hydromagnetic squeeze film lubrication of micropolar fluid between two elliptical plates, *International Journal of Mechanical Engineering and Technology (IJMET)*, 2018; 9(8):939-947.
- Kalavathi GK, Dinesh PA, Gururajan K. Influence of roughness on porous finite journal bearing with heterogeneous slip/no-slip surface, *Tribology International*, 2016; 102:174-181.
- Larsson R., Höglund E. Numerical Simulation of a Ball Impacting and Rebounding a Lubricated Surface, *ASME, J. of Tribology*, 1995; 117:94-102.
- Rahul AK, Rao PS. Rabinowitsch fluid flow with viscosity variation: Application of porous rough circular stepped plates, *Tribology International*, 2021; 154:106635.
- Roelands CJA, Vlugter JC, Watermann HI. The viscosity temperature pressure relationship of lubricating oils and its correlation with chemical constitution, *ASME Journal of Basic Engineering*, 1963; 601-606.
- Sakim A, Nabhani M, Khelifi M El. Non-Newtonian effects on porous elastic journal bearings, *Tribology International*, 2018; 120:23-33.
- Shah RC, Kataria RC. On the squeeze film characteristics between a sphere and a flat porous plate using ferrofluid, *Applied Mathematical Modelling*, 2016; 40(3):2473-2484.
- Venner CH, Wang J, Lubrecht AA. Central film thickness in EHL point contacts under pure impact revisited, *Tribology International*, 2016; 100:1-6.
- Winkler E. Die lehre von der elasticitaet und festigkeit. Theil 1-2, H. Dominicus, Prag; 1867.
- Yang PR, Wen SZ. Pure Squeeze Action in an Isothermal Elastohydrodynamic Lubricated Spherical Conjunction, Part 1: Theory and dynamic load results, *Wear*, 1991; 142:1-16

NOMENCLATURE

- b reference Hertzian radius at load w_0 (m)
- D_{ij} influence coefficients for deformation calculation
- E' equivalent elastic modulus (Pa)
- G dimensionless material parameter, $\alpha E'$
- h film thickness (m)
- h_0 rigid separation (m)
- h_c central film thickness
- h_{min} minimum film thickness
- H dimensionless film thickness, hR/b^2

k	permeability parameter
K	dimensionless permeability parameter, R^2k/b^4
l	characteristic length of micro-polar fluids, $l = (\gamma/4\mu)^{1/2}$
L	dimensionless characteristic length of micro-polar fluids, lR/b^2
N	coupling parameter, $N = [\chi/(2\mu + \chi)]^{1/2}$
p	pressure (Pa)
p_c	central pressure (Pa)
p_h	reference Hertzian pressure at load w_0 (Pa)
P	dimensionless pressure, p/p_h
r	radial coordinate (m)
R	ball radius (m)
t	time (sec)
T	dimensionless time, tE'/μ_0
v_r, v_z	velocity of lubricant in r and z directions, respectively (m/s)
u, w	velocity of lubricant in r and z directions, respectively (m/s)
v_c	normal velocity of ball's center (m/s)
V_c	dimensionless normal velocity of ball's center, $v_c\mu_0R/E'b^2$
ψ	load (N)
Ψ	dimensionless load, $\psi/E'R^2$
X	dimensionless radial coordinate, r/b
z	axial coordinate
z'	pressure-viscosity index
α	pressure-viscosity coefficient
μ	viscosity of lubricant (Pa-s)
μ_0	viscosity at ambient pressure (Pa-s)
$\bar{\mu}$	dimensionless viscosity, μ/μ_0
ρ	density of lubricant (kg m^{-3})
ρ_0	density of lubricant at ambient pressure (kg m^{-3})
$\bar{\rho}$	dimensionless density of lubricant, ρ/ρ_0
Δ	elastic deformation (m)
$\bar{\Delta}$	dimensionless elastic deformation, $R\Delta/b^2$
δ	porous layer thickness (m)
$\bar{\delta}$	dimensionless porous layer thickness, $R\delta/b^2$

多孔介質層及微極性潤滑劑之複合效應之暫態擠壓彈液動潤滑研究

朱力民

國立臺東大學綠能與資訊科技學系

張簡才萬

國立勤益科技大學機械工程學系

張育斌

崑山科技大學機械工程學系

摘要

本研究以數值分析的方式計算解析微極性潤滑劑在具孔隙介質接觸表面受彈性球體定負荷擠壓過程之暫態等溫彈液動潤滑的油膜、壓力、速度分佈值。根據達西定律及艾林根的微極流變理論以圓柱座標模式推導暫態修正雷諾方程式，再使用有限差分法、連續過度鬆弛法及高斯-賽德爾迭代法耦合解析暫態修正雷諾方程式、潤滑劑流變方程式、力平衡方程式、彈性變形方程式。數值模擬結果顯示，多孔介質層的影響相當於吸收潤滑劑，因此油膜厚度減少。微極性潤滑劑的作用相當於提高潤滑劑黏度，因此在暫態純擠壓過程中油膜厚度會增大。由於油膜厚度隨時間的變化，因此在固定載重條件下不同區域的壓力分佈會發生變化，本研究討論多孔介質層的厚度與滲透性以及微極性潤滑劑的特徵長度與偶合參數對暫態彈液動潤滑擠壓特性的影響。

